METEOROLOGICAL APPLICATIONS OF FRACTAL ANALYSIS

by

Michael E. Rocha

B. A., University of California at Los Angeles
(1980)

Submitted to the Department of
Earth, Atmospheric and Planetary Sciences
in Partial Fulfillment of the Requirements for the

Degree of

MASTER OF SCIENCE

at the

MASSACHUSETTS INSTITUTE OF TECHNOLOGY

Signature of Author _____
Department of Earth, Atmospheric
and Planetary Sciences, May, 1984

Certified by: _____
Professor Frederick Sanders
Thesis Supervisor

Accepted by: _____
Professor Theodore R. Madden
Chairman, Departmental Committee
on Graduate Students

METEOROLOGICAL APPLICATIONS OF FRACTAL ANALYSIS

by

Michael E. Rocha

Submitted to the Department of Earth, Atmospheric, and Planetary Sciences in May, 1984 in partial fulfillment of the requirements for the Degree of Doctor of Science in Atmospheric Sciences

ABSTRACT

Fractal analysis was utilized in a manner similar to Lovejoy (1982) to investigate atmospheric scale selectivity. Midlatitude cloud and precipitation areas associated with baroclinic, convective and baroclinic/convective regimes were examined. In addition, 500 mb isohypse and isotherm fields were studied on a seasonal basis. Results from the midlatitude cloud and precipitation data were similar to Lovejoy's findings for analogous tropical structures: fractal analysis indicates no scale selection for atmospheric phenomena with horizontal length scales between ≈ 10 and 10^3 km. The upper level data, however, indicate a change in regime at $\approx 10^4$ km. This may be interpreted as representing the change from synoptic scale forcing mechanisms to planetary scale dynamics.

Thesis Supervisor: Dr. Frederick Sanders

Title: Professor of Meteorology

TABLE OF CONTENTS

BACKGROUND

The research delineated in this paper utilizes a relatively new mathematical concept, that of the 'fractal.' This neologism was coined by its creator, Benoit B. Mandelbrot, about eight years ago and is derived from the Latin adjective fractus, meaning broken (a fairly apt label, as will be seen).

The determination of an object's fractal character is based upon a comparison of its topological dimension, D_T, to its Hausdorff Besicovitch dimension, D. The topological, or Euclidean, dimension of an object is a familiar notion: a line has a Euclidean dimension of one, et cetera. The Hausdorff Besicovitch dimension (more commonly referred to as the fractal dimension) is not quite as straightforward. In practice there are two methods of calculating D. The first involves a comparison of measurements of an object's perimeter made at different resolutions. The finer the precision of measurement, the larger the perimeter. The fractal dimension is represented by the slope of a plot of perimeter versus resolution. The rougher the outline of the object, the more sensitive its perimeter value is to the measurement resolution and, hence, the greater its fractal dimension. The second procedure consists of a comparison of the perimeter versus area values for a set of shapes. It utilizes the formula:

$$P \propto A^{D/2}$$

where P = perimeter

A = area

D = fractal dimension

This is analogous to the previous method described, with the resolution of measurements on a single object being replaced by the area values for a set of geometrically similar objects. In this case the fractal dimension is proportional to the slope of a plot of perimeter versus area values. A change in the fractal dimension implies a breakdown in the geometric similarity assumption, which can be interpreted as representing the transition between two different physical processes.

A shape is said to be a 'fractal' if its fractal dimension is greater than its topological dimension. It can readily be seen that for simple shapes such as circles and squares the fractal dimension is equal to the Euclidean dimension. Hence, these objects are not fractals. But, for any more complicated forms the fractal dimension tends to be greater than the Euclidean dimension, thus qualifying them for Mandelbrot's classification as fractals. Generally speaking, the more contorted the outline of an object is, the larger the value of its corresponding fractal dimension. The Brownian motion of a particle represents an extreme case (in fact, the limiting case) of this contortion. If the particle's path were traced out in two

dimensions it would eventually fill the entire plane. Thus its trajectory, which has a Euclidean dimension of one (that of a line), has a fractal dimension of two (that of a plane). The outlines of most objects found in nature lie somewhere between the simplicity of circles and squares and the complexity of Brownian motion trajectories. Hence, their associated fractal dimensions range from one to two. This points out a useful aspect of fractal analysis: implementation of it makes it possible to precisely quantify the dimensional chacteristics of any given shape in terms of a non-integral value, as opposed to being constrained to the very general integral values of the Euclidean dimension. So the calculation of D gives one the ability to distinguish between forms that were heretofore lumped into the same topological category. This analytic sensitivity is especially important in the examination of the complex spectrum of shapes that occurs in the natural world.

The question now arises as to the applicability of fractal analysis. Of what importance is it to have a more refined determination of an object's dimensionality? Mandelbrot's first applications of the fractal dimension involved the examination of a hodgepodge of naturally occurring as well as man-made forms ranging from soap bubbles to Koch curves. His calculations demonstrated the flexibility of this anlysis to topologically categorize virtually any shape. This categorization is scientifically useful if a given physical process has its own unique value of D. This is intuitively reasonable since it seems likely that the geometric characteristics of

structures resulting from different processes would not be the same. Using this idea Mandelbrot showed the role his new concepts played in the study of specific problems in physics, most notably those involving turbulent processes. He suggests that fractal analysis may yield some useful information concerning the boundaries between different regions of turbulent flows. These boundaries, whichmost likely constitute a fractal set, could be quantitatively categorized in terms of the fractal dimension. The next step would be to theoretically determine the physical significance of the fractal dimension values and variations (if any) that are found. This approach would hopefully aid in the interpretation of phenomena such as intermittency, in which highly turbulent flows contain scattered quiescent regions. In addition, fractal analysis may be applied to the solutions of the Euler or Navier/Stokes equations for turbulent flows, in that the singularities of these flow fields may be a fractal set. Other aspects of turbulent flows such as particle trajectories and imbedded vortices may also prove to be fractals, indicating that fractal analysis might be useful in their examination. Mandelbrot also hypothesizes that the flow associated with clear air turbulence is a fractal set. This leads us to the application of fractal analysis to meteorological studies. The first attempt at this was made quite recently be S. Lovejoy (1982). He examined fairly high resolution satellite and radar data from the Indian Ocean region and calculated the fractal dimensions of cloud and precipitation areas. His results indicate that D for both of these quantities is

approximately four-thirds and that this value does not vary significantly over six orders of magnitude in area.

These findings have some interesting implications. First, the fact that D turned out to be four-thirds may have some physical significance in itself, although Lovejoy does not offer any speculation on this [it should be noted that Kolmogoroff's minus five-thirds power law predicts a fractal dimension of four-thirds for isobars]. Secondly, these results imply that tropical cloud and precipitation areas have no preferred horizontal length scale, as indicated the scale independence of D.

This is somewhat disturbing in that it is generally assumed that atmospheric processes are associated with characteristic spatial dimensions. Specifically, results from research concerned with the determination of the atmospheric kinetic energy spectrum point to the existence of different energy regimes for different scales. Julianet alii (1970) used wind data in their examination of the energy spectrum and found a k^{-3} dependence (k being the wavenumber) for systems with wavenumbers ranging from approximately six to twenty. Desbois (1972) used covariance functions to analyze Southern Hemispheric wind data and found that this -3 dependence continued out to approximately wavenumber thirty-five. By compiling data from a number of wind variability studies, Gage (1979) extended this analysis to smaller scales and found a $k^{-5/3}$ variation for disturbances having wavelengths $\lesssim$1000 km. The combined result of these studies, then, is that the kinetic energy of the troposphere exhibits a $k^{-5/3}$

dependence at small scales and a k^{-3} dependence at larger scales with a transition occurring at a horizontal length scale of about 1000 km. A -5/3 wavenumber dependence is indicative of a three-dimensional isotropic regime while a -3 dependence indicates a two-dimensional regime. Gage's data show that the three-dimensional regime extends well into the mesoscale, something that seems rather unusual. He hypothesizes that this extension refects the existence of a two-dimensional reverse energy cascade, with energy flowing upscale and enstrophy flowing downscale, the opposite of three-dimensional transfer. The energy transfer is associated with a $k^{-5/3}$ spectrum and the enstrophy transfer with a k^{-3} spectrum. Actually, this idea of the existence of a two-dimensional inertial subrange was not new; it was originally postulated by Kraichnan (1967). Steinberg (1972) had questioned the validity of explaining the -3 wavenumber dependence in terms of a two-dimensional, isotropic flow. He argued that in the wavenumber range $7 \leq k \leq 15$ the flow is not two-dimensional since the dominant energy conversion (eddy available to eddy kinetic) is three-dimensional and is also not isotropic at scales this large. He suggested instead that the agreement between Kraichnan's theory and the actual data may be coincidental and proposed that the -3 dependence may be associated with the imaginary part of the wave phase speed. This hypothesis is based on purely dimensional grounds, namely that the dominant spectral parameter has the dimension inverse time. Desbois (1972) expressed a similar doubt as to the applicability of two-dimensional inertial theory to waves in the $7 \leq k \leq 15$ range,

pointing out that the flow is not truly inertial due to its close proximity to the excitation wavelength of baroclinic instability. Gage, however, found it reasonable to use this two-dimensional flow assumption to explain the results of spectral studies and suggests that phenomena such as individual thunderstorms, wind shear, breaking waves, et cetera represent the small-scale source of the energy that is two-dimensionally transferred upscale. Lilly (1983) examined this proposal by analyzing the wakes of moving bodies in stratified flows. These wakes evolve in much the same way as the processes suggested by Gage as being associated with the mesoscale energy profile and thus provide a means of testing the reverse energy cascade hypothesis in the laboratory. Lilly found that initially three-dimensional isotropic turbulence divides into approximately equal parts of gravity waves and quasi-two-dimensional turbulence in the presence of strong stratification. The gravity waves propagate away from the source while the two-dimensional turbulence propagates to larger scales and is responsible for the wavenumber dependence seen in the mesoscale portion of the horizontal kinetic energy spectrum, thus lending credence to Gage's hypothesis. Charney (1971) showed theoretically that the -3 wavenumber dependence for $7 \leq k \leq 20$ can be explained in three-dimensional terms by considering the conservation of pseudo-potential vorticity, analogous to the conservation of vorticity in two-dimensional systems.

At any rate, the gist of all of these studies is the existence of preferred length scales for particular atmospheric phenomena.

Lovejoy's initial results seem to provide a counterexample, although it appears as if the quantities he examined did not extend out to large enough scales to exhibit the dimensional transition found in the wind variability studies. Later work by Schertzer and Lovejoy (1983) expands upon the idea that atmospheric processes have no characteristic length scales, specifically that there is no transition from three-dimensional to two-dimensional flow patterns as one goes from small to large scales. Instead, they hypothesize the existence of a single dimensional parameter for all scales, something they refer to as the 'elliptical dimension.' This quantity is somewhat analogous to Mandelbrot's fractal dimension, although instead of comparing the perimeter to the area of an object, it involves a three-dimensional comparison of its horizontal and vertical dimensions. It gets its name from the fact that it quantifies the transition from small-scale elliptical eddies with major axes in the vertical to large-scale elliptical eddies with major axes in the horizontal. The elliptical dimension ranges from two (for flat objects) to three (for spherical objects). Schertzer and Lovejoy show empirically and theoretically that the atmosphere has an elliptical dimension value of 23/9 ($\approx$2.56), indicative of the fact that it consists of flow patterns that are somewhere between flat and spherical.

As of now it appears as if no definitive conclusions can be drawn as to scale selection (if any) of atmospheric motions or the dynamical reason behind any such scaling. Energy spectrum studies are limited by the paucity of wind data and the inherent errors associated with

interpolation or covariance calculations. Fractal analysis offers another method of determining the scale of atmospheric processes.

In the present work, an analysis similar to Lovejoy's (1982) is made of midlatitude cloud and precipitation areas. Also, in an effort to extend fractal analysis to larger scales, hemispheric height and temperature fields are examined.

DATA ANALYSIS

Four meteorological parameters were examined: cloud outlines obtained from enhanced infrared satellite imagery, precipitation areas from radar maps, 500 mb height contours and 500 mb isotherms. The satellite and radar data of nine individual episodes were analyzed--three from each of the following categories: (1) baroclinic/convective, (2) convective, and (3) baroclinic. The baroclinic/convective cases involve synoptic-scale cyclones containing what appear to be a significant number of convective cells. The baroclinic episodes consist of synoptic-scale cyclones associated with a minimal amount of convection and the convective cases involve no large-scale disturbances, only relatively large numbers of convective cells. The baroclinic/convective situations were chosen with the idea in mind that these events had a reasonable chance of exhibiting a spatial dependence in the fractal dimension--a phenomenon not observed in the tropics. Individual convective cells tend to be small in comparison with rather expansive cirrus cloud shields associated with mature baroclinic cyclones. Assuming that a given physical process results in a type of cloud mass with a particular fractal dimension value, the small-scale cloud elements should have a fractal dimension representative of convective processes while the larger cloud shields should be associated with a dimension characterisitic of baroclinic phenomena. To contrast the hybrid baroclinic/convective cases, purely

convective and purely baroclinic situations were also examined. It was hypothesized that these episodes would each yield a different value of the fractal dimension.

Satellite Imagery

Cloud data were acquired from GOES-East enhanced infrared DB5 satellite photos. The enhancement begins with the -32°C isotherm--id est, any cloud top with a blackbody temperature $\leq$-32°C appears as a flat gray on the satellite picture. A different shade of gray (the scale actually ranges from white to black) is used for every ≈10°C increment below -32°C. In this study only the -32°C contour was utilized. This choice was made somewhat arbitrarily, with convenience being a not unimportant factor. There is some physical justification in examining this particular isotherm, however, as it has been found to correlate fairly well with precipitation regions (Scofield and Oliver, 1977). Hence, these cloud areas may be thought of as corresponding to the physical process of precipitation and their associated fractal dimension value may then be directly compared with that obtained from radar map data. It may also be argued that these cloud regions reflect mid-tropospheric latent heat and advection patterns, an interpretation that may lead to more far-ranging implications. With the adoption of this viewpoint, the exact value of temperature used as a contour outline becomes relatively unimportant. In a previous investigation of this sort (Lovejoy, 1982),

the -10°C isotherm was used in the examination of tropical cloud masses. It was found that varying this threshold temperature from -5°C to -15°C did not appreciably alter the results.

The areal coverage of the satellite pictures used in this investigation included basically the eastern United States and a portion of the western North Atlantic: from approximately 25 to 55 degrees north latitude and 65 to 95 degrees west longitude. The resolution of the enhanced imagery is eight kilometers.

The two quantities of interest in the determination of an object's fractal dimension are its area and its perimeter. Hence, measurements of these parameters were made for each of the relevant cloud masses found in the nine cases that were examined. Measurements were made by hand, as digitized satellite imagery was unavailable. A polar planimeter was used to determine areal values and a map measurer was employed to measure perimeters. Actually, even though the crudeness of the measuring devices limited the effective resolution of the data, this would not affect the determination of the fractal dimension, a fact which seems counter-intuitive. This can be understood when it is realized that D is basically the slope of a log-log plot of perimeter versus area. Thus, a change in resolution, which would result in a change in the perimeter values, would not alter the slope of a log perimeter versus log area graph and, hence, would not affect D for a given set of data. Rather, poor resolution associated with crude measurements would show up as an increase in the

standard deviation of the data from a straight line fit.

The analysis of Case I will serve as a general example of the techniques used. Figure 1 shows the cloud outline transcribed from the satellite imagery. In addition to the -32°C contour, the -52°C isotherm was included as well. It was felt that this representation of higher cloud tops may be of interest, especially in convective situations. Measurements of this contour can be used as a consistency check for the results obtained from the -32°C outlines, or they may aid in the determination of the vertical variation of the fractal dimension, if any. Table I lists the corresponding perimeter and area values for each of the cloud mass outlines. The graphical representation of these data is shown in figure 2. A line was best-fit to the set of points and the fractal dimension was determined from the slope of this line; here, the fractal dimension is equal to twice the slope. The standard deviation and correlation coefficient were also computed.

The perimeter versus area graphs for the remaining baroclinic/convective episodes (cases II and III) and the convective episodes (cases IV, V and VI) are shown in figures 3 through 7; the baroclinic episodes (cases VII, VIII and IX) were not analyzed on an individual basis as each case had a rather sparse number of data points and it seemed as if any line derived from such a limited number of values would be subject to sampling error.

An examination of figures 2 through 7 reveals that the data of each episode constitute an extremely linear set over approximately

ØØZ 3 April 82

FIGURE 1 Cloud mass outlines. outer contours: -32°C
inner contours: -52°C

• 25° N, 70° W

TABLE I

Satellite Imagery 0000 GMT 3 April 1982

Cloud Mass #	Perimeter	Area
1	6570 km	696000 km^2
2	580	9000
3	360	3600
4	90	600
5	80	500
6	80	400
7	80	600
8	50	300
9	230	2800
10	570	8300
11	910	9700
12	840	22100
13	170	2200
14	10440	1343200
15	310	5200
16	60	600
17	90	1100
18	100	500

TABLE I (continued)

Cloud Mass #	Perimeter	Area
19	440 km	10000 km^2
20	160	2000
21	50	500
22	170	600
23	150	2300
24	120	900
25	50	200
26	60	300

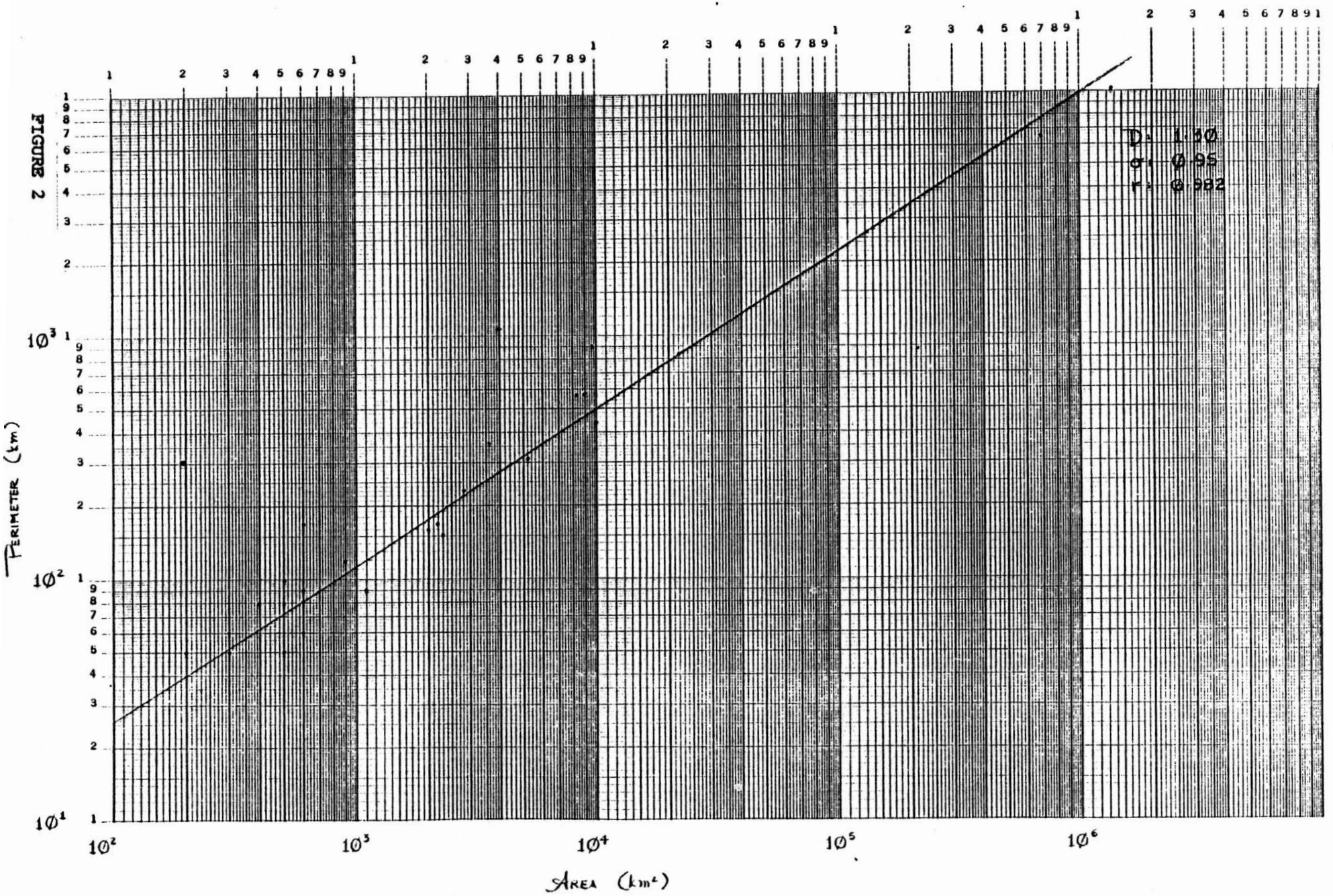

FIGURE 2

CASE I
002 3 APRIL 72

20

SATELLITE

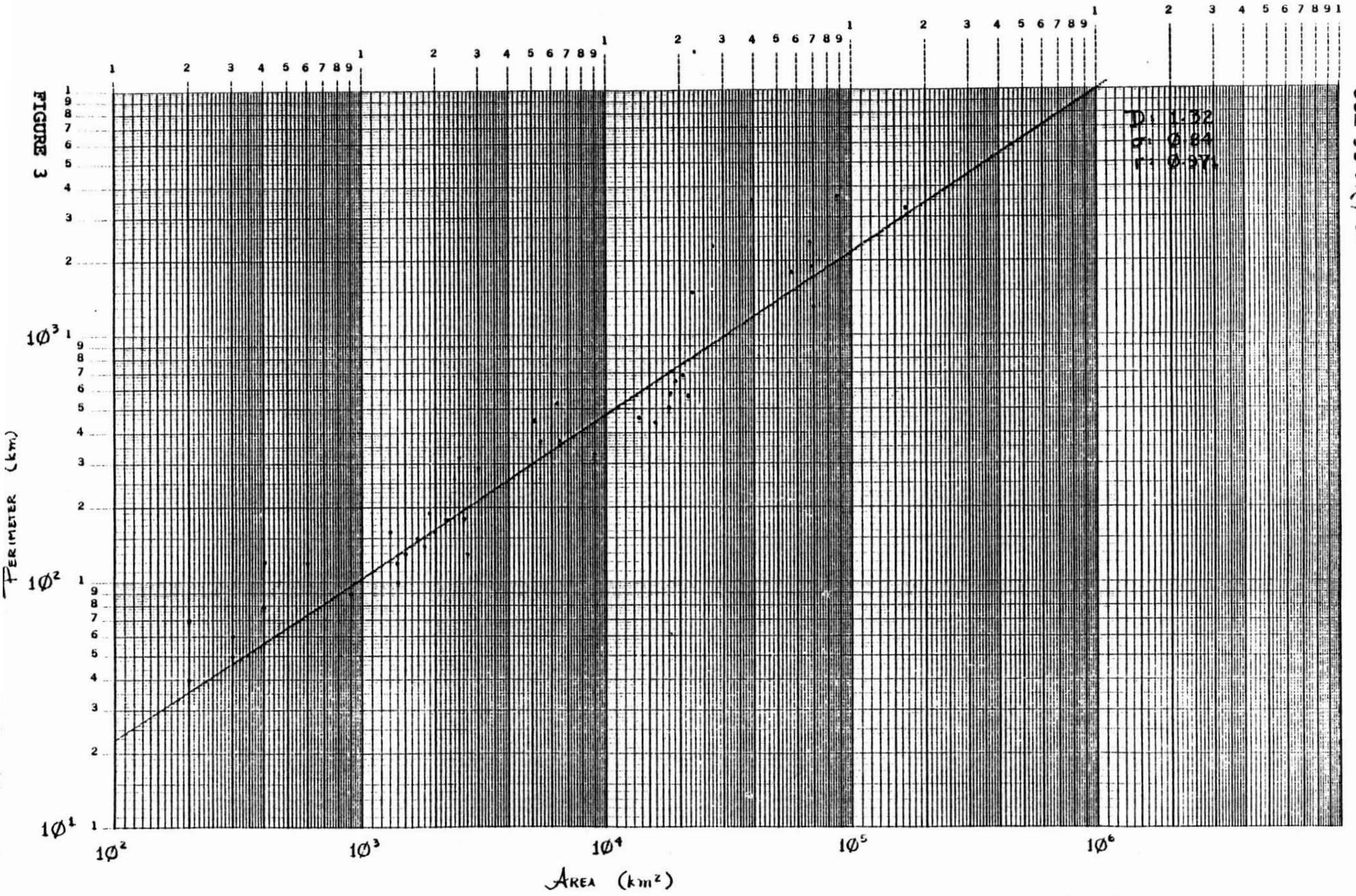

FIGURE 3

CASE II
002 30 May 82

21

SATELLITE

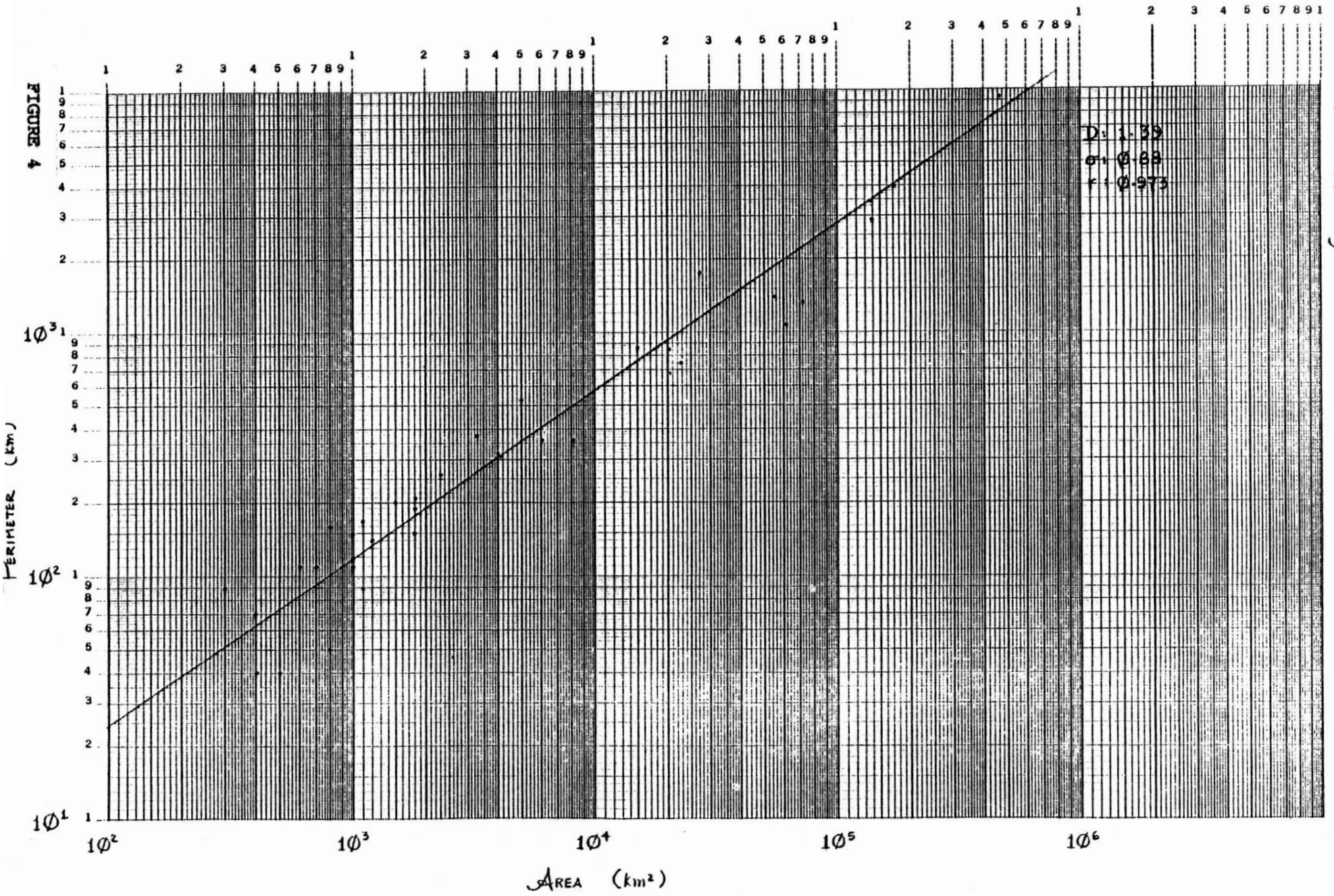

FIGURE 4

CASE III
002 8 April 73
22
SATELLITE

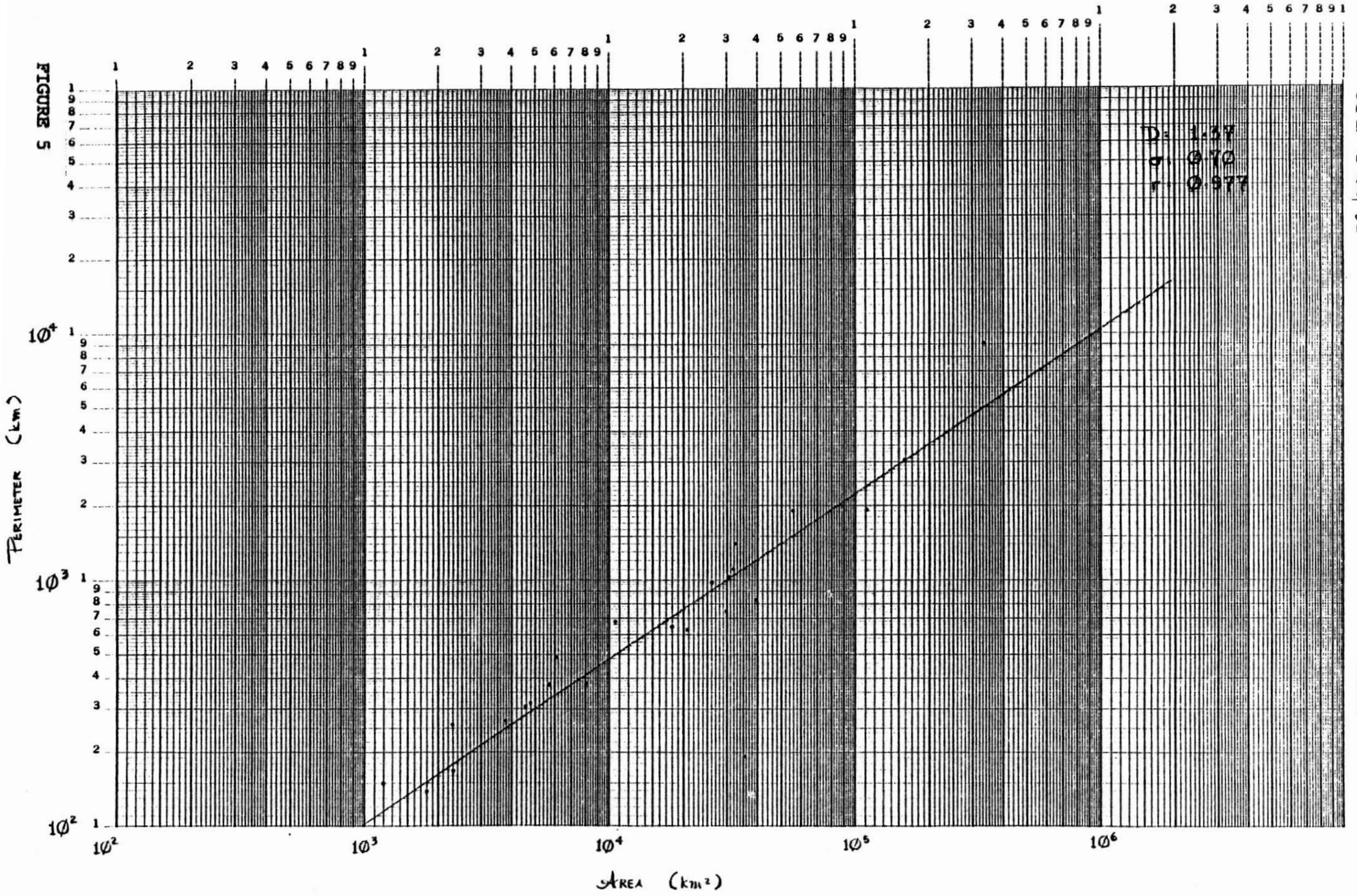

FIGURE 5

CASE IV

Ø1 Z 1 July 72

SATELLITE

FIGURE 6

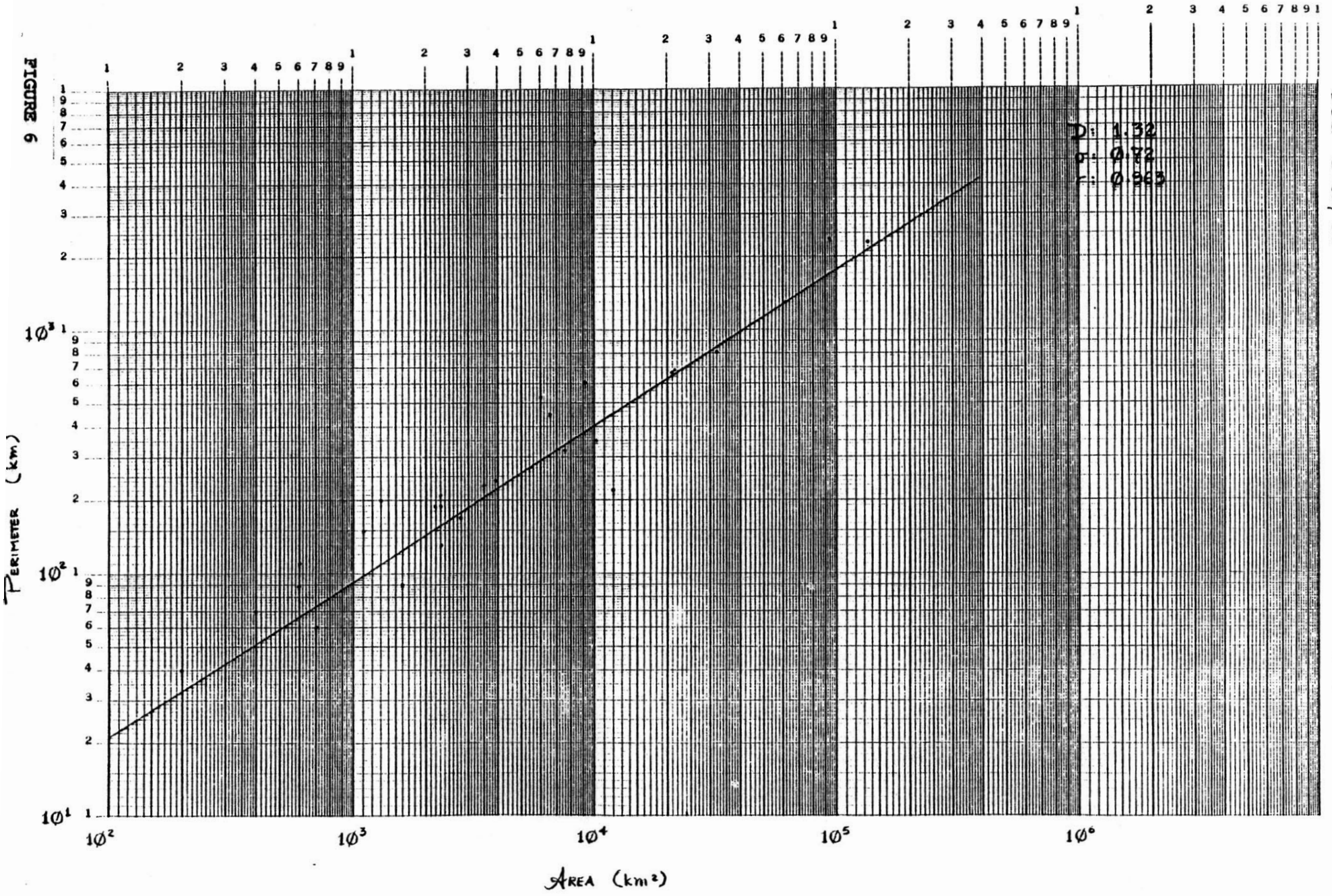
PERIMETER (km)
AREA (km²)
1Ø¹
1Ø²
1Ø³
1Ø⁴
1Ø⁵
1Ø⁶
CASE V
ØØZ 2 July 72
SATELLITE
24

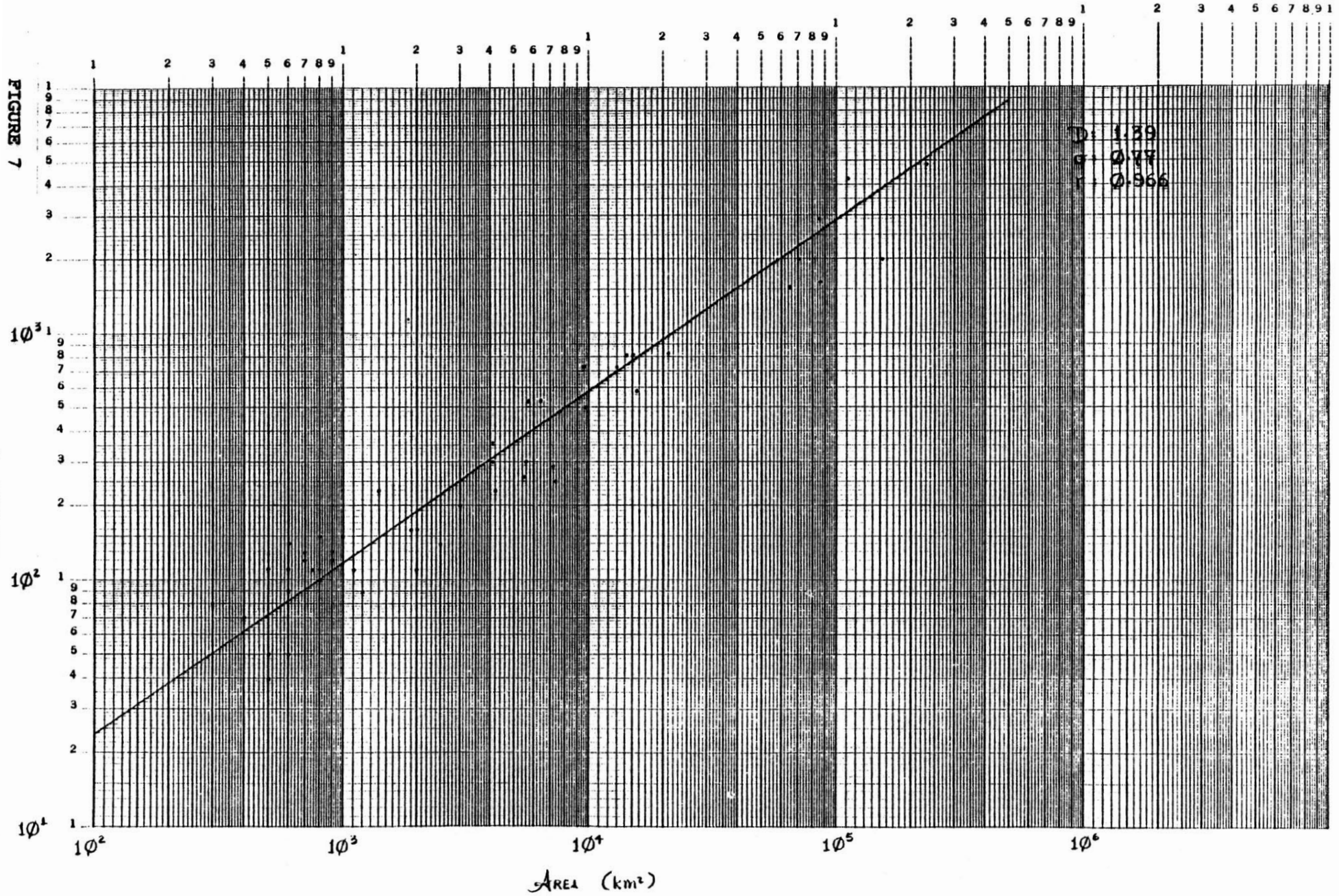

FIGURE 7

CASE IV
002 3 JULY 72

25

SATELLITE

four spatial orders of magnitude. The correlation coefficients are consistently high and the standard deviations are rather low. It was hypothesized that the baroclinic/convective cases would exhibit a variation of the fractal dimension with size, possibly even a discontinuity between the small-scale convective regime and the large-scale baroclinic regime. This definitely does not appear to be so. In addition to the high degree of linearity, the data of case I through VI exhibit very consistent values of the fractal dimension, all within a few percent of the four-thirds value obtained previously in the study of tropical cloud masses.

The measurements from the three cases representing each meteorological regime were compiled and appear in figures 8 through 10. The fractal dimension value obtained from the three baroclinic occurrences is noteworthy in that it deviates noticeably from four-thirds; it is closer to three-halves. Although the correlation coefficient of this data set is very high, the somewhat limited amount of measurements makes one hesitant about drawing any conclusions as to the significance of this deviation. Actually, the fact that the fractal dimension associated with the baroclinic episodes differs appreciably from that found in the baroclinic/convective cases may not be as important as the result that the convective episodes have the same fractal dimension as the baroclinic/convective cases.

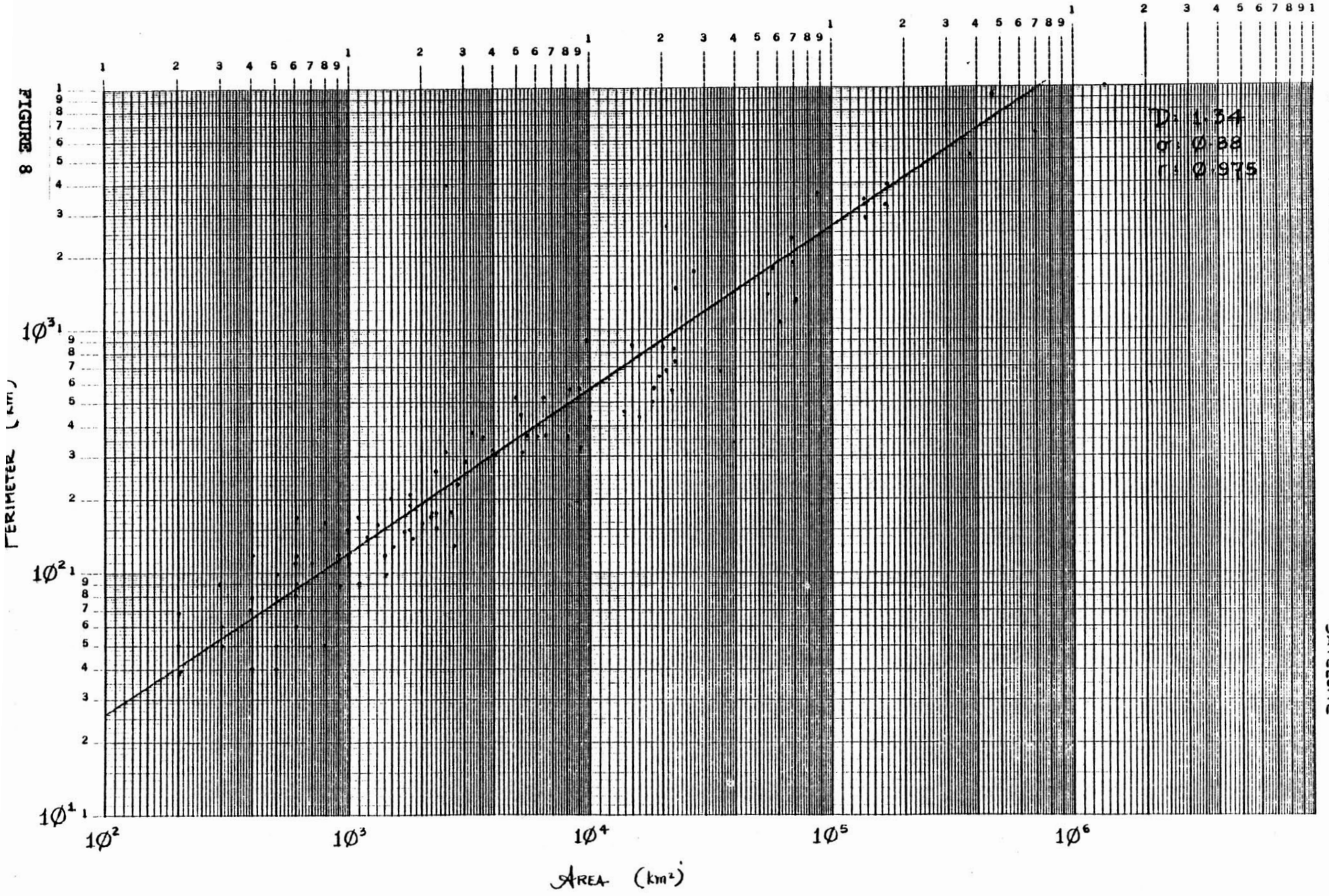

FIGURE 8

CASES I, II & III

SATELLITE

FIGURE 9

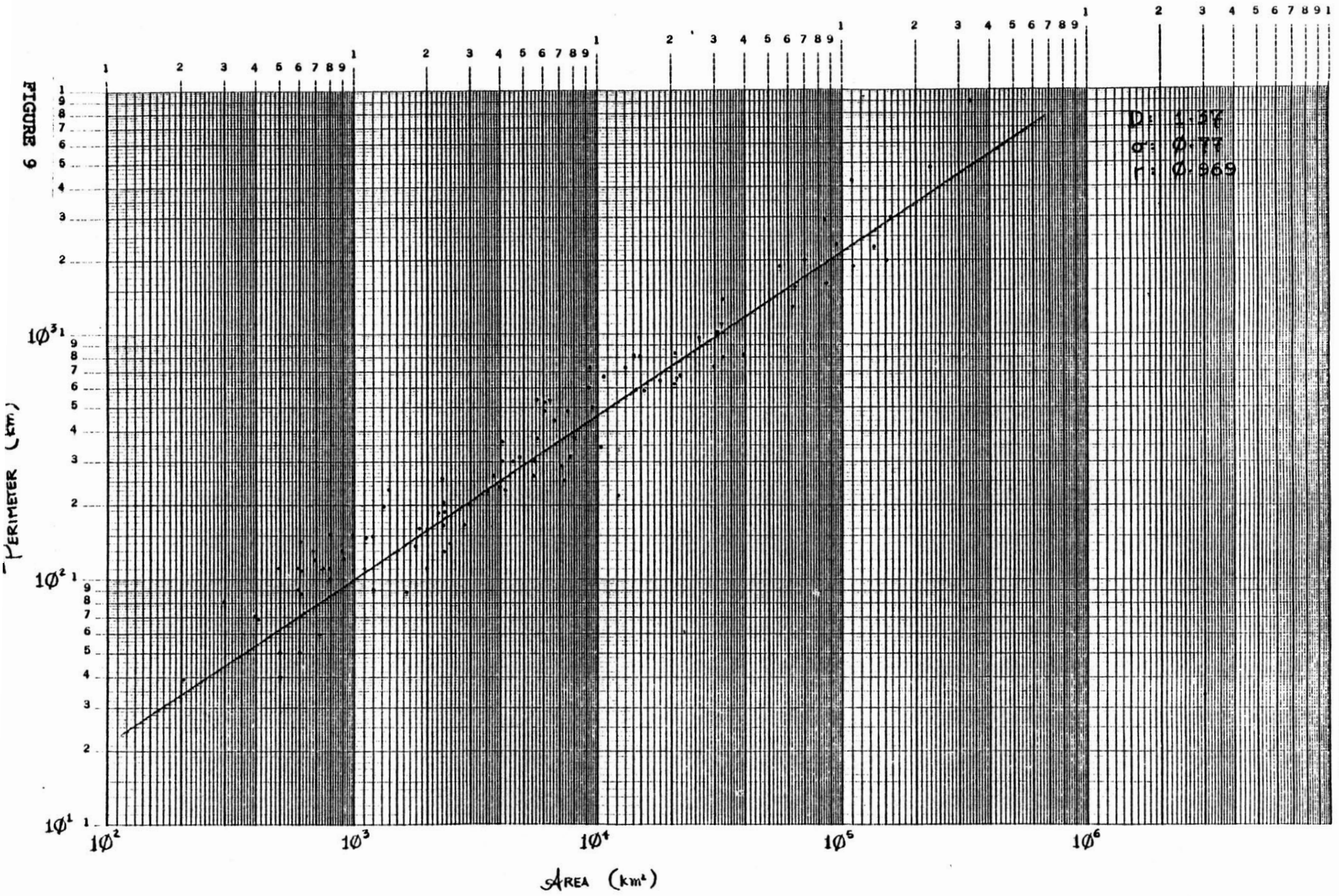

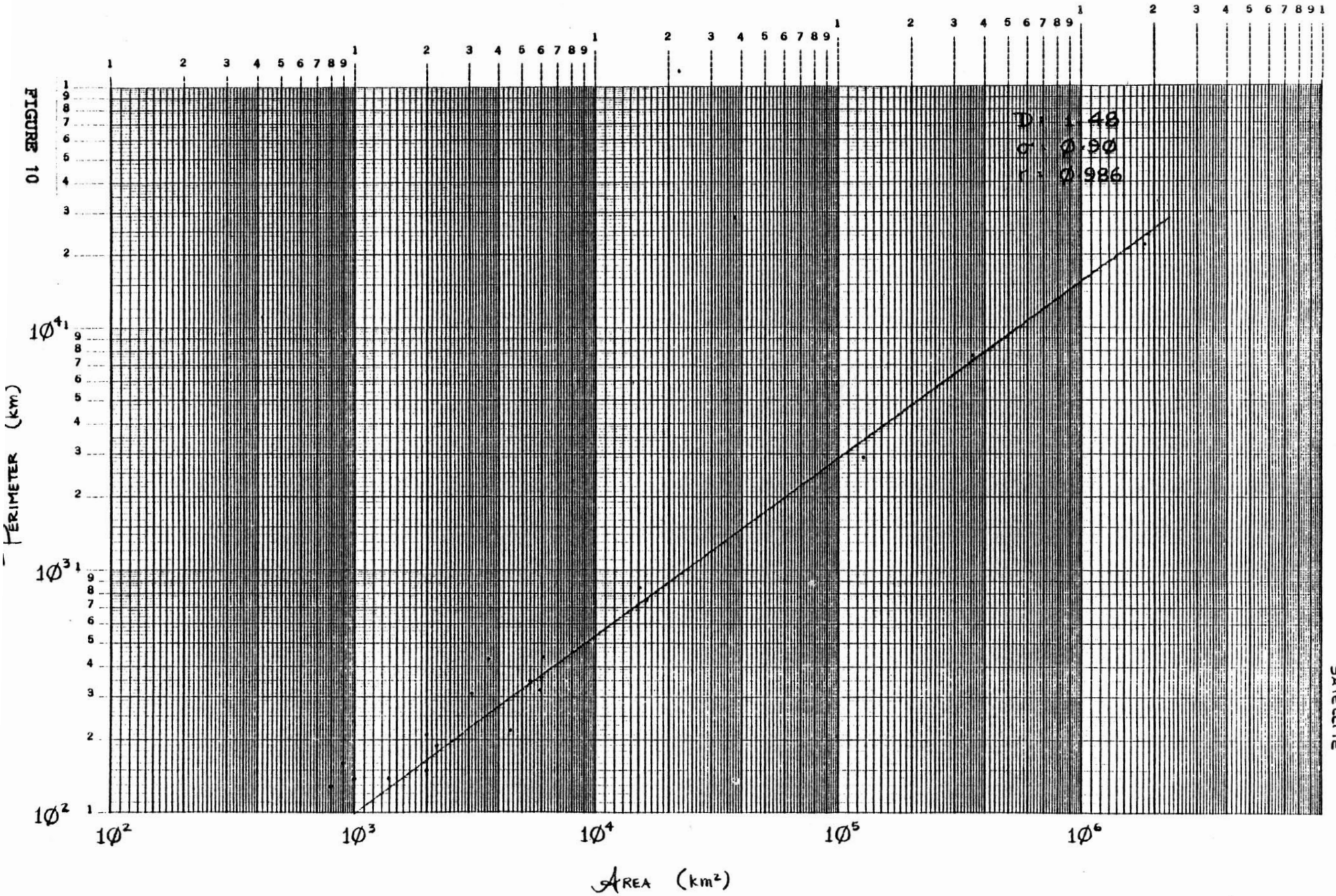

FIGURE 10

CASES VII, VIII & IX

SATELLITE

Radar Maps

Data for this part of the study were derived from hourly National Meteorological Center radar maps. These maps delineate precipitation areas and contour discrete VIP (vertically integrated precipitation) levels corresponding to particular ranges of precipitation intensity. In this investigation the VIP level one isopleths were examined, which represent the boundary between precipitation and precipitation-free regions. Analogous to the analysis of the satellite imagery, it may be worthwhile to go back and investigate the fractal properties of higher VIP level contours.

The analysis used on these maps was the same as that used on the satellite photos. Although the coverage of the radar maps included the entire United States, only the area corresponding to that of the DB5 satellite pictures was utilized in order that these two data sets might be directly compared.

Figures 11 through 13 show the perimeter versus area graphs for the compilations of the three individual episodes comprising each of the three different types of regimes studied. Due to the relatively low number of measurements associated with a given case, an examination of each episode individually was not considered to be statistically meaningful. The results of these compilations are somewhat different than those gleaned from the satellite cloud masses. First, the overall fractal dimension of the radar map VIP regions is somewhat higher than that of the cloud masses. Its

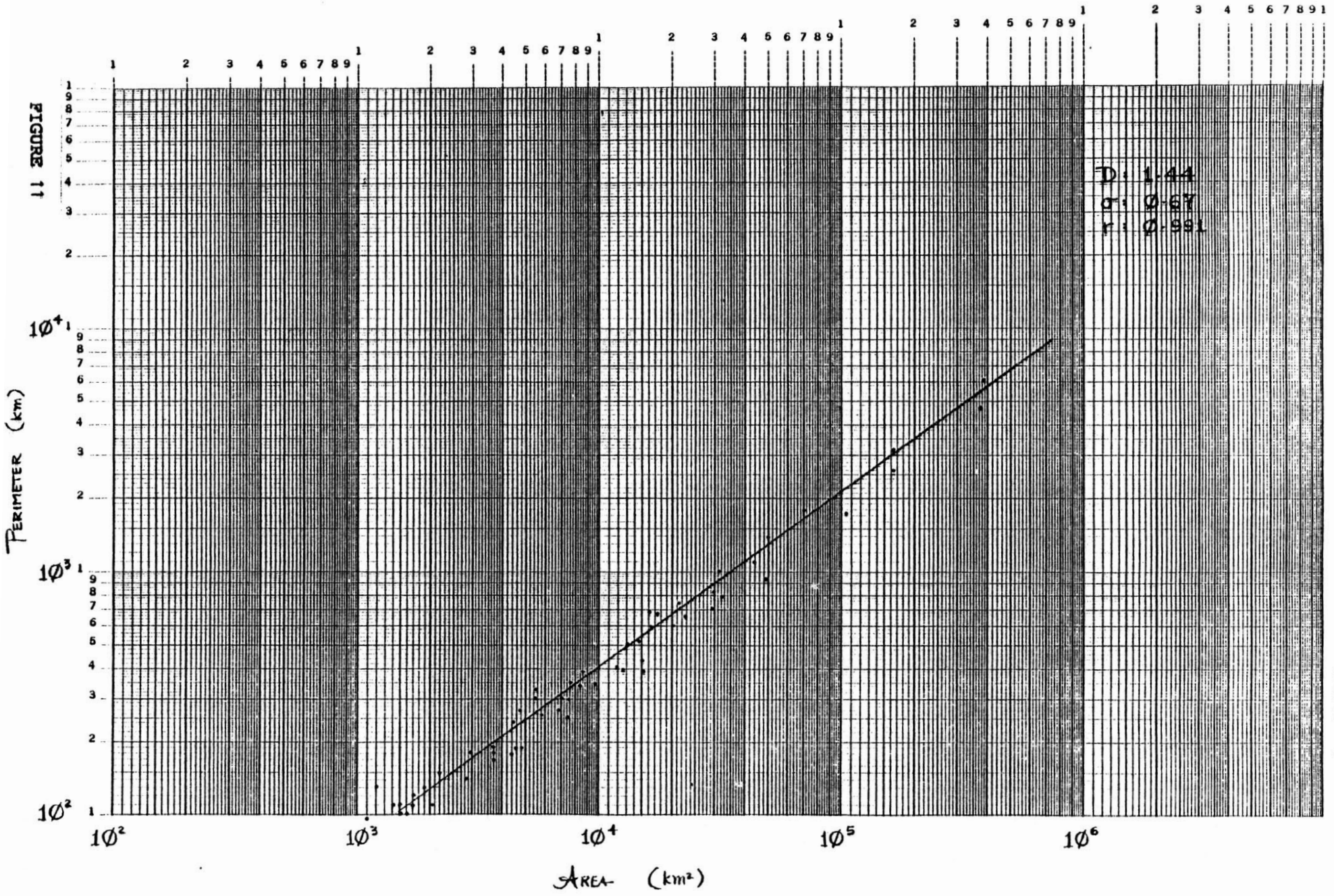

FIGURE 11

CASES I, II & III

RADMAPS

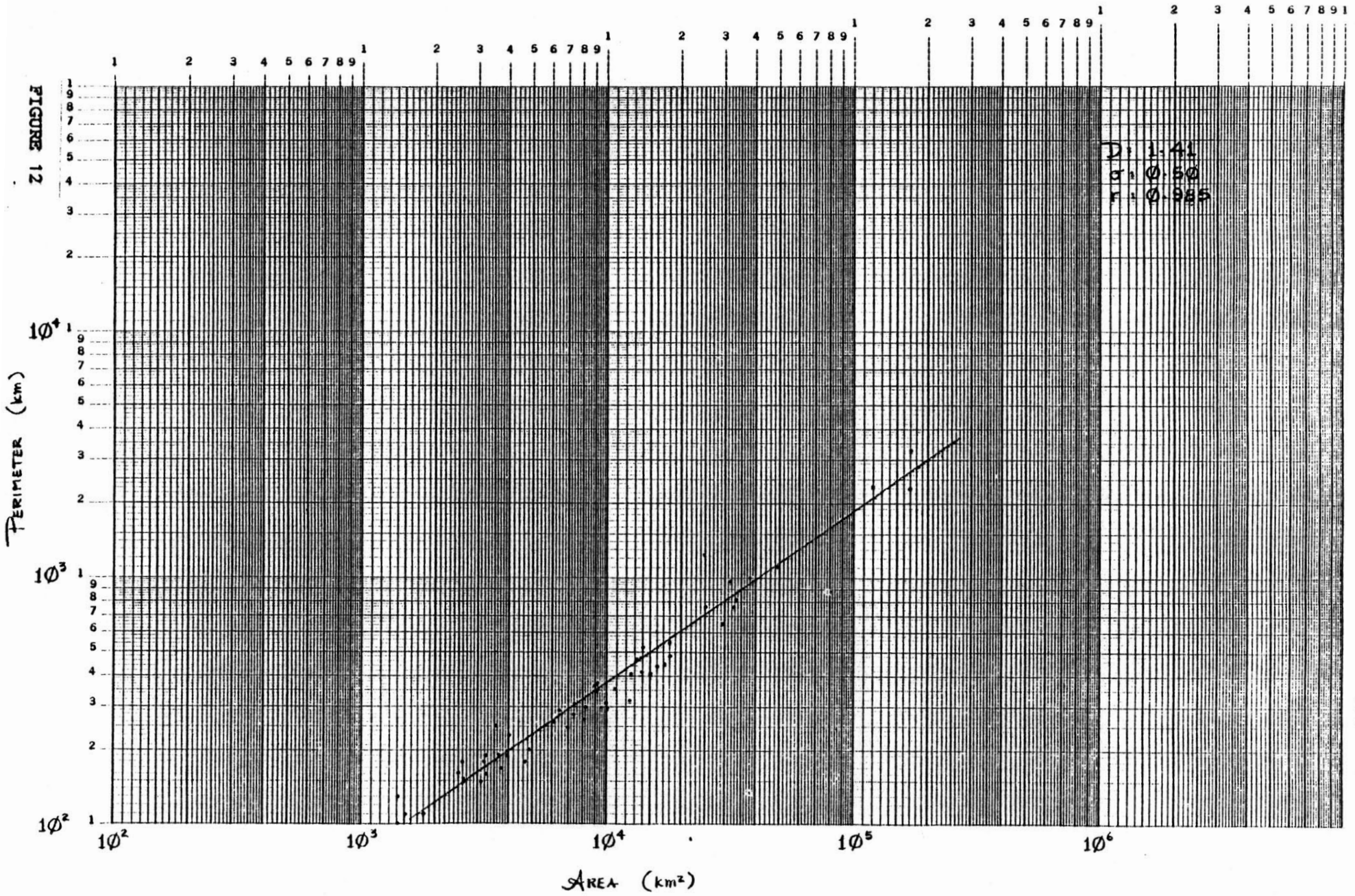
PERIMETER (km)
AREA (km²)
1Ø²
1Ø³
1Ø⁴
1Ø⁵
1Ø⁶
CASES IV, V & VI
RADMAPS

FIGURE 12

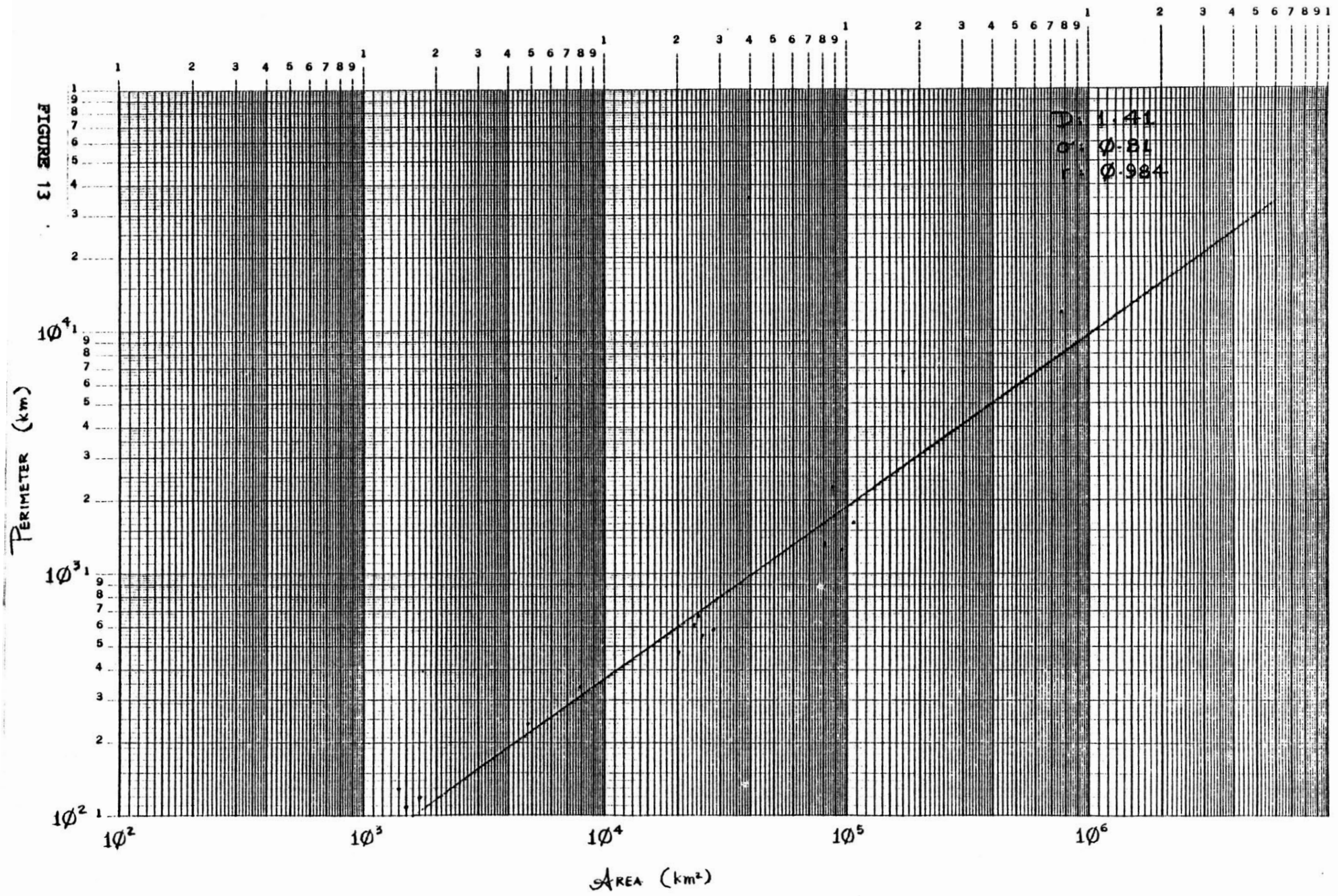

FIGURE 13.

value is also more consistent from one type of episode to another--the radar data do not exhibit a higher value of the fractal dimension in the baroclinic regime as was the case with the satellite data. An important similarity in the two data sets is the lack of any sort of a 'kink' in the graphs; the radar echo measurements do not appear to exhibit any spatial dependence of the fractal dimension over approximately three orders of magnitude.

500 mb Charts

The maps used were NMC's 0000 GMT 500 mb analyses. These charts were of interest in that they display meteorological quantities on a large scale, making it possible to extend the fractal analysis to contours encompassing larger areas.

Two types of isopleths were analyzed; isohypses (lines of constant height), in six dekameter intervals and isotherms, in 5°C intervals. Since the flow at 500 mb is to a good approximation in geostrophic balance, the shape of the isohypses corresponds well with the wind field. Hence their fractal properties can, in a crude sense, be related to the advective patterns of the flow field, as can the fractal properties of the cloud masses that had previously been analyzed. The fractal characteristics of the isotherm configurations can also be linked with those of the cloud masses, as well as the radar echoes, since all of these quantities are directly related to the spatial distribution of latent heat release.

The 500 mb isohypses for four time periods--January, April, July and October 1983 (representing each season of the year) were examined using the previously delineated analysis procedure. Five maps per month, at weekly intervals, were utilized. This temporal spacing was felt to be advantageous for comparing individual episodes, as day-to-day variations of flow patterns at this level tend to be relatively small. For the January charts, height contours ranging from the lowest on a given map out to 552 dkm were measured. Although the 552 dkm contour correlates approximately with the core of the jet stream at this time of year, its choice as an upper-bound involved more pragmatic considerations than physical ones (the planimeter used to determine areas is limited as to the size of what it can measure). By July the circumpolar vortex has significantly contracted, thus allowing measurements of contours with values as high as 582 dkm, although for this study the meaningful aspect of a contour is its areal extent, not its actual height.

Figures 14 through 17 show the perimeter versus area graphs for each month's isohypses. The calculated fractal dimension of these isopleths is quite a bit smaller than the values associated with the cloud mass and precipitation area contours. This simply reflects the fact that the height contours are somewhat smoother--id est, the perimeter enclosing a given area is smaller. This implies that the shape of the height lines is more circular and/or less convoluted than the cloud mass and precipitation outlines. In this case it's most

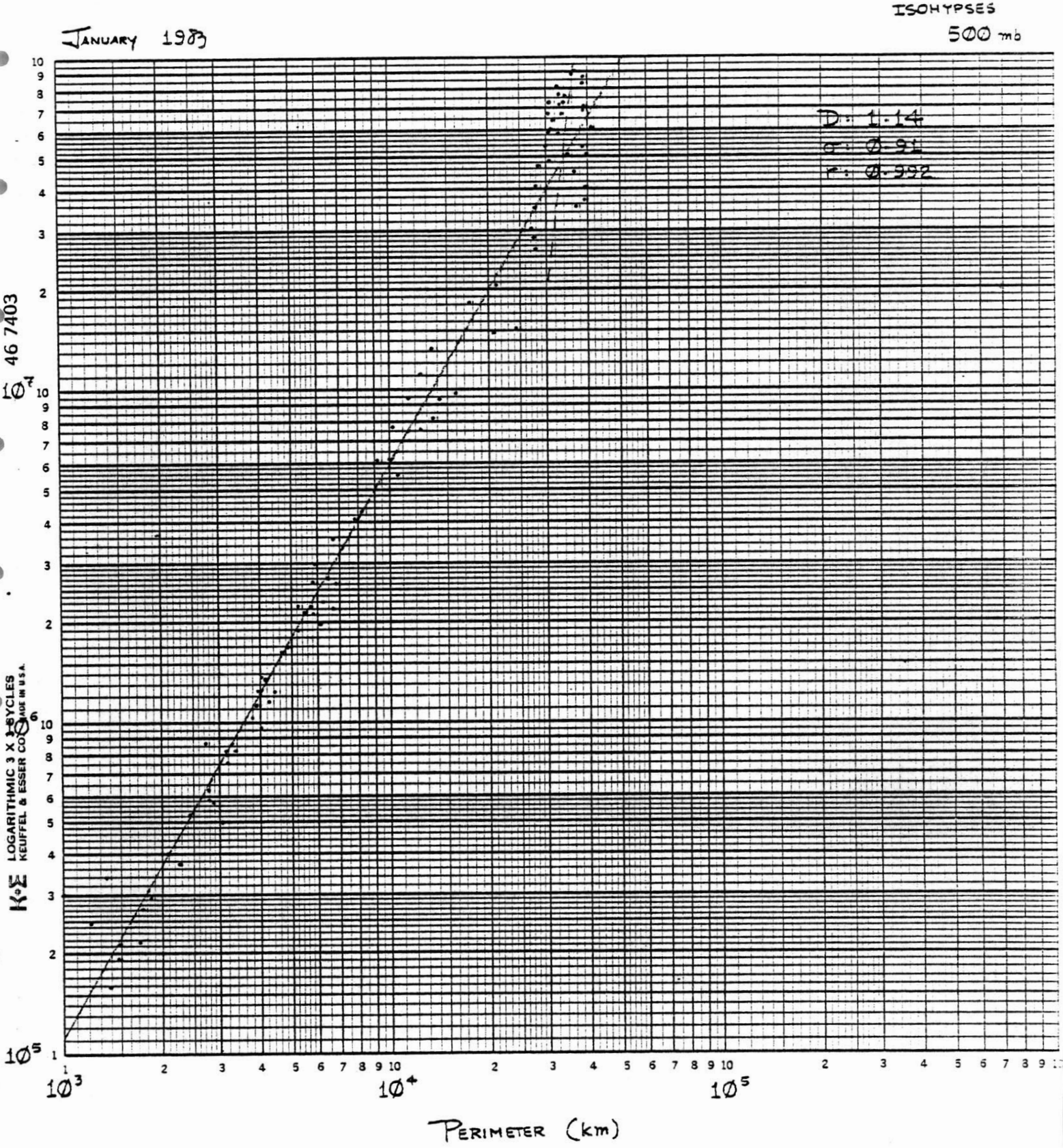
ISOHYPSES
500 mb
JANUARY 1983
D: 1.14
σ: 0.91
r: 0.992
AREA (km²)
PERIMETER (km)
LOGARITHMIC 3 X 1 CYCLES
KEUFFEL & ESSER CO. MADE IN U.S.A.
46 7403

FIGURE 14

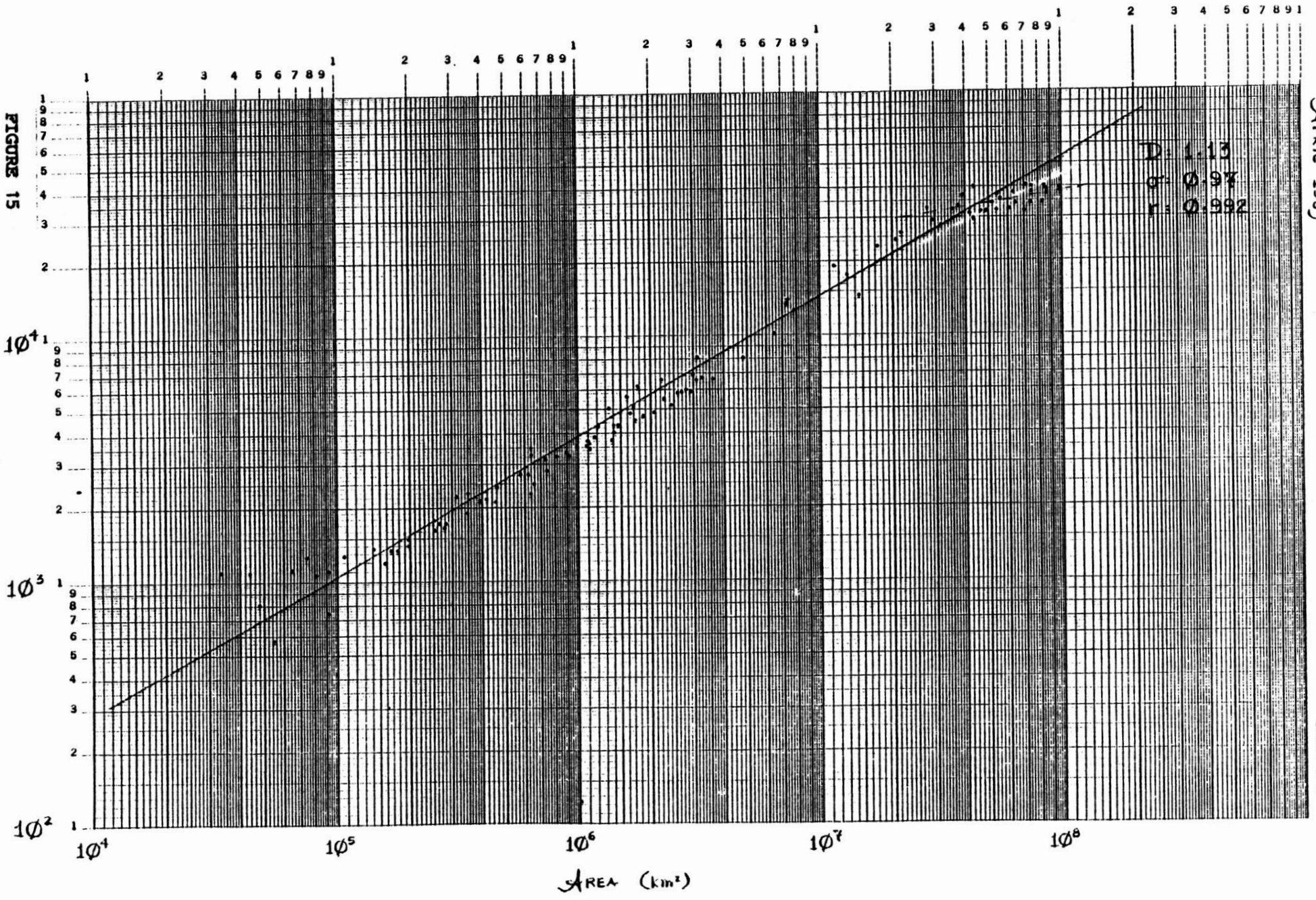

FIGURE 15

APRIL 1973

ISOHYPSES 500 mb

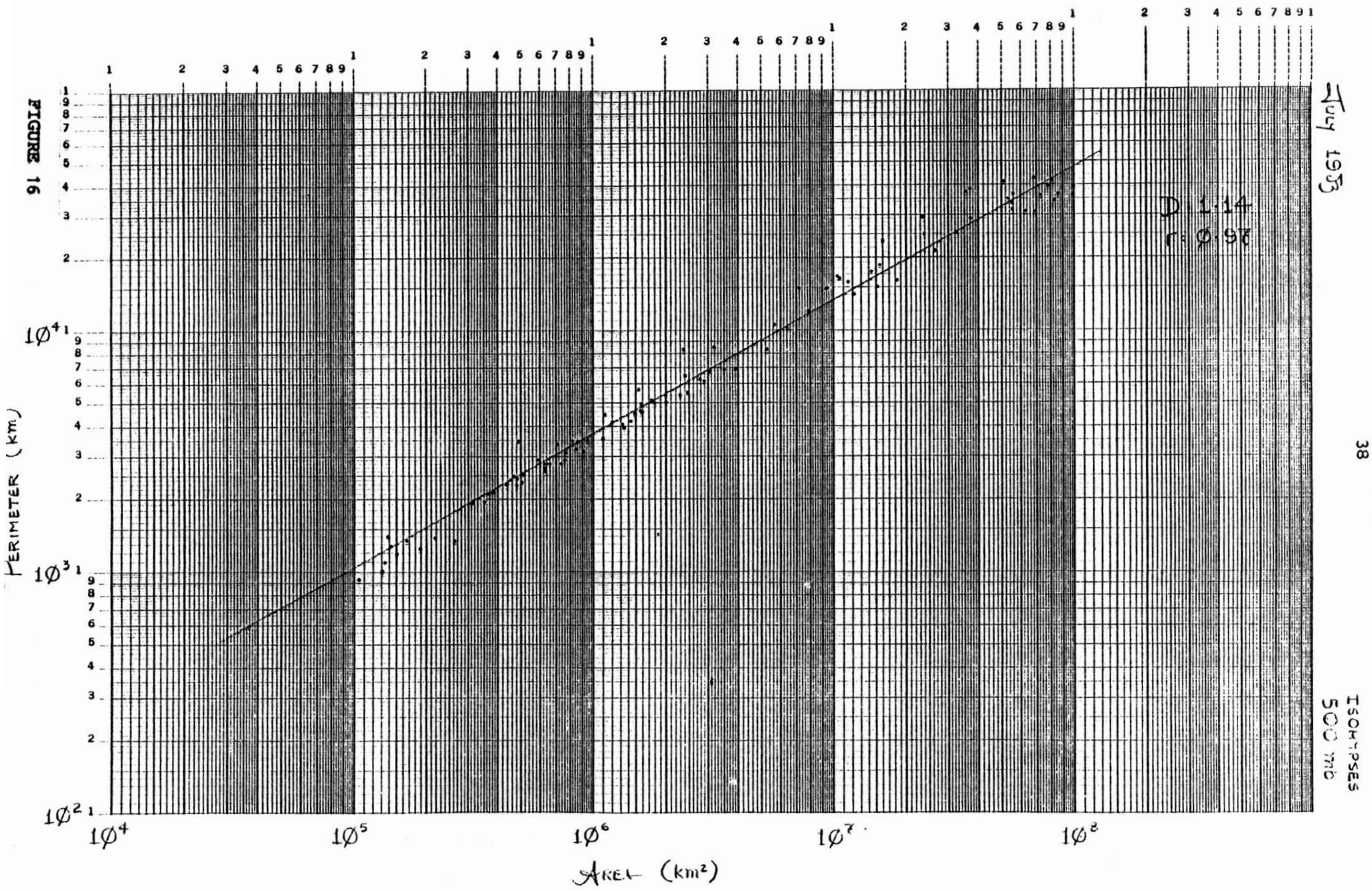

FIGURE 16

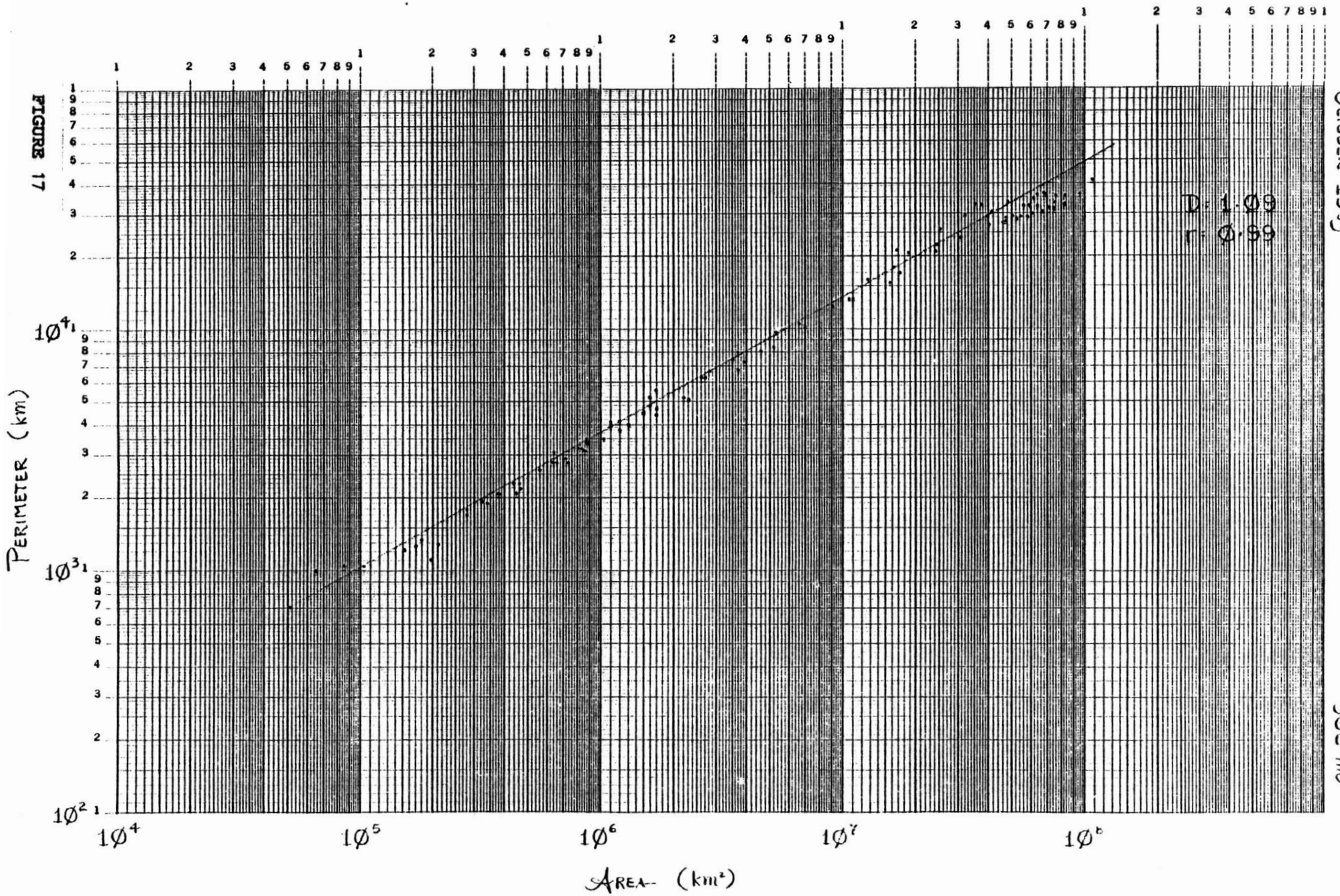

FIGURE 17

OCTOBER 1973

39

ISOHYPSES
500 mb

likely a combination of these two factors. Physically, the difference in fractal dimension could be interpreted as representing the difference between large-scale (synoptic and planetary) and small-scale (mesoscale and convective) processes.

An important difference between the isohypse data and the cloud mass/precipitation area data is the presence in the former of a distinct 'kink' in the perimeter versus area graphs at large scales. This deviation in slope occurs at $\approx 2.5\text{-}3.0 \times 10^7$ km^2 (corresponding to a perimeter of $\approx 3 \times 10^4$ km) and represents a significant change in the fractal dimension value. Table II shows the quantification of this. Slope and fractal dimension values were recalculated separately for contours encompassing areas greater than and less than $\approx 2.5 \times 10^7$ km^2. The change in D at large scales is most likely associated with a shift from a spatial regime characterized by relatively circular cut-off features to a larger scale regime characterized by undulating circumpolar flow. This is a noteworthy result in that it is the first evidence of the spatial dependence of the fractal dimension on an episodic basis. A result that is somewhat surprising is that the isohypse fractal dimension does not appear to have a significant seasonal dependence. Intuitively it would seem as if D should be lower in the spring and autumn, when cut-off features are more prevalent. Actually, the October data did have a relatively low fractal dimension value, but the April flow patterns did not.

The results from the isotherm analyses are shown in figures 18 and 19. In January, the perimeter versus area plot has

TABLE II

Alternate Best Fits

Date	Parameter	Perimeter	Area	D
1/83	Isohypses	$<2.5\times10^4$ km	$<2.5\times10^7$ km^2	1.20
		$>2.5\times10^4$	$>2.5\times10^7$	1.00
	Isotherms	$<3.0\times10^4$	$<3.0\times10^7$	1.20
		$>3.0\times10^4$	$>3.0\times10^7$	1.08
4/83	Isohypses	$<2.5\times10^4$	$<2.5\times10^7$	1.16
		$>2.5\times10^4$	$>2.5\times10^7$	0.88
7/83	Isohypses	$<2.5\times10^4$	$<2.0\times10^7$	1.18
		$>2.5\times10^4$	$>2.0\times10^7$	1.13
	Isotherms	$<3.0\times10^4$	$<3.0\times10^7$	1.34
		$>3.0\times10^4$	$>3.0\times10^7$	1.03
10/83	Isohypses	$<2.5\times10^4$	$<2.5\times10^7$	1.13
		$>2.5\times10^4$	$>2.5\times10^7$	0.92

FIGURE 18

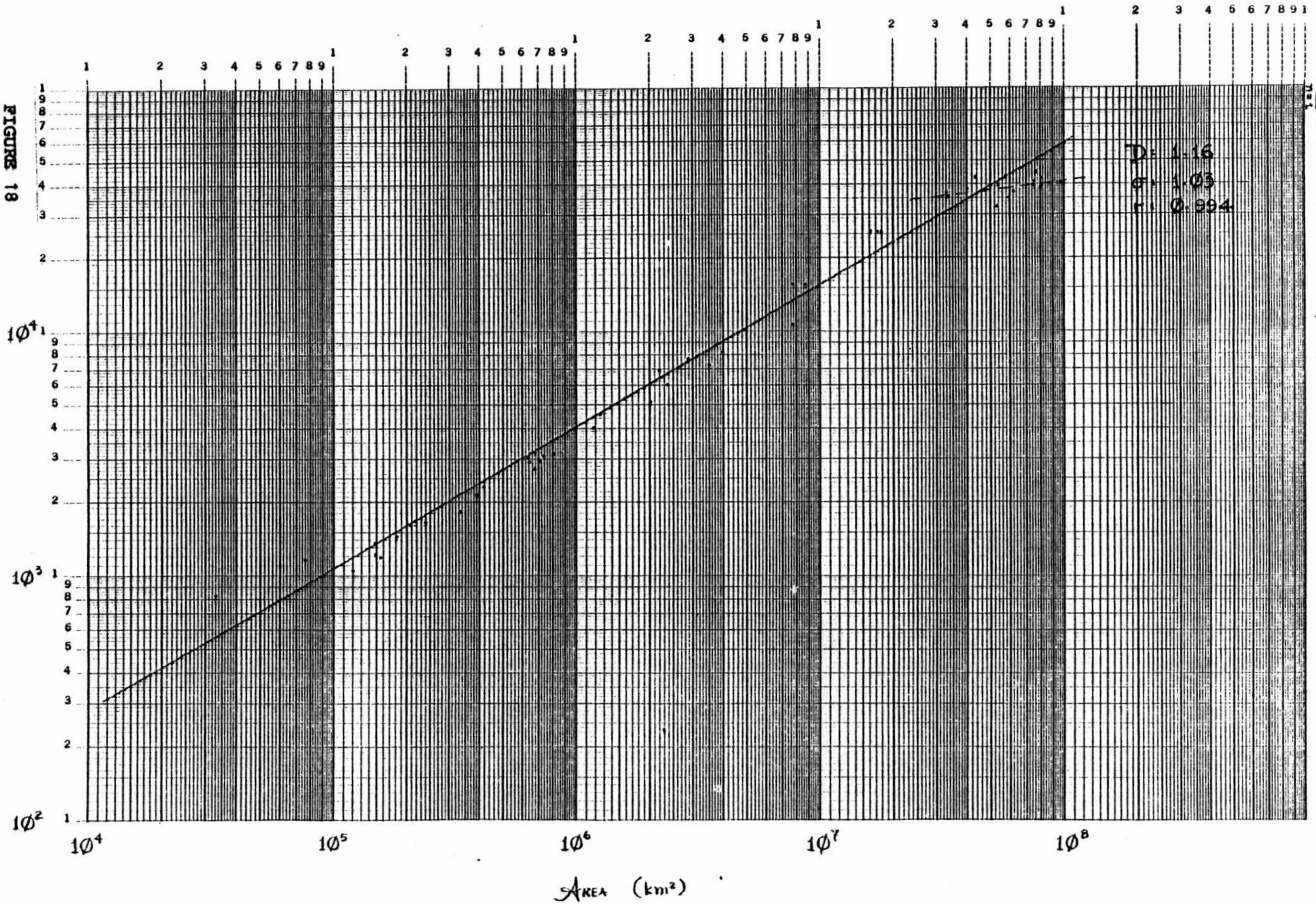

500 mb (7h-6) JANUARY 1958

ISOTHERMS

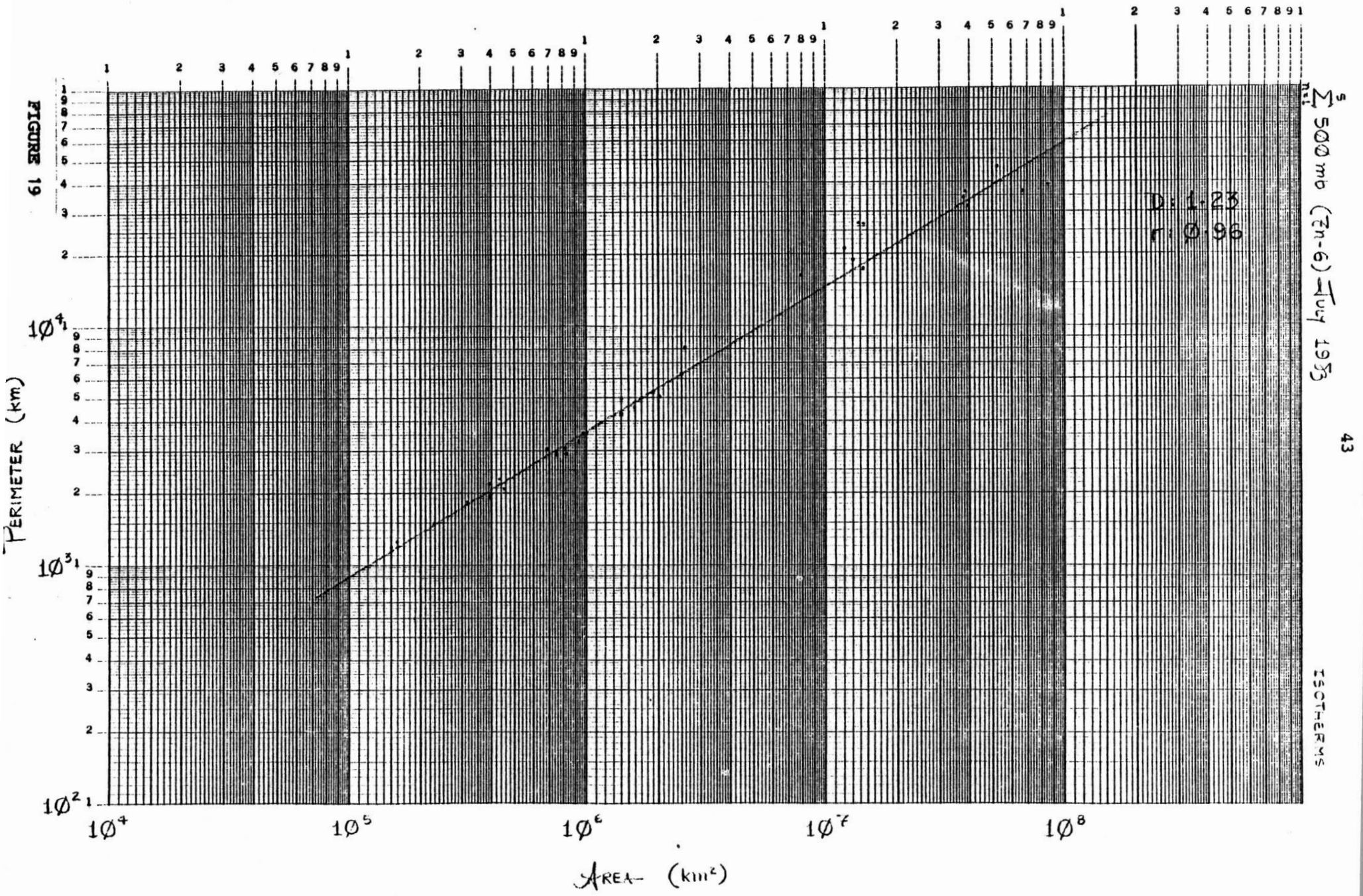

FIGURE 19

characteristics that are quite similar to the corresponding isohypse graph--specifically, a very linear relationship between log A and log P values, with a distinct discontinuity at large scales. In July, the hemispheric temperature gradient is much smaller and, hence, the number of isotherms is significantly less. Thus, there are correspondingly fewer data points. What values there are seem to indicate that there may not be a large-scale fractal dimension discontinuity during the summer. The July isohypse graph also hints at this.

SUMMARY AND CONCLUSIONS

In this study an extension has been made of the work done by S. Lovejoy (1982). His investigation involved the application of fractal analysis in the determination of atmospheric scale selection. He examined the fractal properties of tropical cloud masses and precipitation areas and could find no evidence of any scale selectivity. The present research dealt with midlatitude cloud masses and precipitation areas as well as analyses of 500 mb flow patterns and temperature fields.

Three different types of meteorological conditions were chosen in the examination of cloud masses and precipitation areas: baroclinic, convective, and baroclinic/convective, in order to adequately test for the presence of scale selection. 500 mb data were incorporated into the study so that the characteristics of larger scale phenomena could be analyzed. Isohypses and isotherms were examined on a seasonal basis.

It was found that a fractal dimension analysis of midlatitude cloud mass and precipitation area data yielded no sign of any atmospheric scale selection, the same result obtained by Lovejoy in his examination of tropical data. This was surprising in that it was hypothesized that the presence of different dynamic processes in midlatitudes (namely, convective and baroclinic) operating at supposedly different scales would be associated with structures whose geometric properties varied accordingly with scale. It can thus

be concluded that either the atmosphere is not scale-selective out to structures with areal extents of $\approx 10^6$ km^2 or there is a flaw in Mandelbrot's premise that different phenomena give rise to objects with different spatial characteristics, and hence different values of his fractal dimension.

In terms of the absolute value of the fractal dimension, the cloud masses from the convective and baroclinic/convective cases were associated with a D of ≈4/3, similar to Lovejoy's findings. The clouds from the purely baroclinic episodes yielded a data set with a significantly higher fractal dimension value--close to 3/2. Assuming that cloud masses resulting from purely convective processes and cloud masses resulting from purely baroclinic processes have different fractal dimension values (as indicated by these results), the fact that the hybrid baroclinic/convective situations had an associated fractal dimension comparable to the convective cases indicates that convection may be the dominant structural determination mechanism out to scales well beyond the size of individual convective elements. This result agrees with Gage's (1979) finding, based on data compiled from a number of wind variability studies, that the three-dimensional isotropic regime extends well into the mesoscale.

The precipitation area data had an associated fractal dimension that was apparently higher than that derived from the cloud mass information, but was actually comparable when the fact that the resolution of the radar measurements was greater than that of the satellite picture measurements was taken into account.

Unfortunately, a physical interpretation of the significance of the particular value of the fractal dimension associated with a given structure is 'beyond the scope of this paper.'

The results obtained from the analysis of the 500 mb isohypse and isotherm data deviate significantly from Lovejoy's findings in that they definitely illustrate some sort of atmospheric scale selectivity (assuming, at least, that the basic premise involved in the interpretation of fractal dimension data is correct). A fairly well-defined change in D occurs at a horizontal scale of $\approx 3 \times 10^4$ km, corresponding to structures with planetary wavelengths. This deviation occurs in all seasons, although it appears to be less well-defined during the summer. It could possibly represent the transition from synoptic scale forcing mechanisms to planetary scale dynamics. This result is important in that it indicates that fractal analysis may be a viable tool in the investigation of atmospheric scale selection. Currently, atmospheric energy spectra studies utilize harmonic analyses of wind variability data. Fractal analysis offers another means of interpreting this as well as other types of data.

REFERENCES

Charney, J. G., 1971: Geostrophic turbulence. J. Atmos. Sci., Sci., 28, 1087-1094.

Desbois, M., 1972: Large-scale kinetic energy spectra from Eulerian analysis of EOLE wind data. J. Atmos. Sci., 32, 1838-1847.

Gage, K. S., 1979: Evidence for a $k^{-5/3}$ law inertial range in in mesoscale two-dimensional turbulence. J. Atmos. Sci., 36, 1950-1953.

Julian, P. R., W. M. Washington, L. Hembree and C. Ridley, 1970: On the spectral distribution of large-scale atmospheric kinetic energy. J. Atmos Sci., 27, 376-387.

Kraichnan, R. H., 1967: Inertial ranges in two-dimensional turbulence. Phys. Fluid, 10, 1417-1423.

Lilly, D. K., 1983: Stratified turbulence and the mesoscale variability of the atmosphere. J. Atmos. Sci., 40, 749-761.

Lovejoy, S., 1981: The statistical characterization of rain areas in terms of fractals. Boston Radar Conference preprint.

Mandelbrot, B. B., 1982: The fractal geometry of nature. Freeman, 460 pp.

Schertzer, D. and S. Lovejoy, 1983: The dimension of atmospheric motions. Unpublished. For a copy, write: EERM/CRMD, Meteorologie Nationale, 2 Ave. Rapp, Paris 75007, France.

Scofield, R. A. and V. J. Oliver, 1977: A scheme for estimating convective rainfall from satellite imagery. NOAA Tech. Memo. NESS 86, Washington, D. C., 47 pp.

Steinberg, H. L., 1972: On the power law for the kinetic energy spectrum of large scale atmospheric flow. Tellus, 24, 288-292.